

LEARNING TO RECONSTRUCT SIGNALS WITH INEXACT SENSING OPERATOR VIA KNOWLEDGE DISTILLATION

Roman Jacome[†], Leon Suarez[‡], Romario Gualdrón-Hurtado[‡], Luis Gonzalez[‡], Henry Arguello[‡]

[†]Department of Electrical, Electronics and Telecommunications Engineering

[‡]Department of Systems and Informatics Engineering

Universidad Industrial de Santander, Bucaramanga, Colombia, 680002

ABSTRACT

In computational optical imaging and wireless communications, signals are acquired through linear coded and noisy projections, which are recovered through computational algorithms. Deep model-based approaches, i.e., neural networks incorporating the sensing operators, are the state-of-the-art for signal recovery. However, these methods require exact knowledge of the sensing operator, which is often unavailable in practice, leading to performance degradation. Consequently, we propose a new recovery paradigm based on knowledge distillation. A teacher model, trained with full or almost exact knowledge of a synthetic sensing operator, guides a student model with an inexact real sensing operator. The teacher is interpreted as a relaxation of the student since it solves a problem with fewer constraints, which can guide the student to achieve higher performance. We demonstrate the improvement of signal reconstruction in computational optical imaging for single-pixel imaging with miscalibrated coded apertures systems and multiple-input multiple-output symbols detection with inexact channel matrix.

Index Terms— Single-pixel imaging, MIMO detection, knowledge distillation.

1. INTRODUCTION

In several applications, signals $\mathbf{x} \in \mathbb{R}^n$ are acquired through linear coded and noisy projections $\mathbf{y} \in \mathbb{R}^m$ as following $\mathbf{y} = \mathbf{A}\mathbf{x} + \boldsymbol{\omega}$, where $\mathbf{A} \in \mathbb{R}^{m \times n}$ is the sensing operator and $\boldsymbol{\omega} \in \mathbb{R}^m$ is additive Gaussian noise. Consequently, a reconstruction algorithm is required to retrieve the underlying signal after the acquisition process. This computational sensing framework has opened new frontiers in a wide range of wireless communications [1–3] and imaging applications, including microscopy [4, 5], computational photography [6], and remote sensing [7]. Therefore, recovering the underlying signal is a long-standing and widely studied problem, typically referred to as an (ill-posed) inverse problem. Several methods are based on model-based approaches, algorithms that take into account the sensing model. These methods are formulated as the optimization of a data-fidelity term $f(\mathbf{x})$ aiming to fit the estimated signal to the observed measurements, and a regularizer term $g(\mathbf{x})$ to promote prior information about the signal. The optimization problem is then formulated as

$$\underset{\tilde{\mathbf{x}}}{\text{minimize}} f(\tilde{\mathbf{x}}) + \lambda g(\tilde{\mathbf{x}}), \quad (1.1)$$

This work was supported by project VIE-UIS under the research project 3944 and ICETEX and MINCIENCIAS through the CTO 2022-0716 Sistema óptico-computacional tipo pushbroom en el rango visible e infrarrojo cercano (VNIR), para la clasificación de frutos cítricos sobre bandas transportadoras mediante aprendizaje profundo, desarrollado en alianza con citricultores de Santander, under Grant 8284. Romario Gualdrón acknowledges the support of the IEEE SPS Scholarship.

where λ is the regularization parameter that balances the fidelity and regularization terms. For the regularization term $g(\mathbf{x})$, a plethora of approaches has been proposed such as sparsity, total variation or low-rank [8–10]. While these methods rely on hand-crafted designs of the signal prior, in some practical scenarios, these assumptions are not met leading to subpar performance [11]. Learning-based approaches have also been proposed, where the signal prior is implicitly optimized using a large paired signal-measurement dataset [12]. Mainly, these methods aim to fit a neural network that maps from the measurements to the target signal. The network structure is one of the most important aspects of this kind of recovery method. Commonly used architectures such as convolutional or fully connected neural networks, and transformers, are considered *black boxes* due to their lack of interpretability [13]. Unrolling networks, a model-based neural network, address this issue by providing a hybrid solution that integrates the structured iterative algorithms of model-driven approaches with the adaptability of deep learning, which not only enhances interpretability but also delivers high performance in recovery tasks [13–15]. These model-based methods require a complete knowledge of the sensing operator \mathbf{A} , which in some applications may not be available. In this work, we consider two main applications where this problem is crucial:

Computational optical imaging: In a single-pixel camera (SPC), a coded aperture (CA) (a binary array with values $\{0, 1\}$ or $\{-1, 1\}$) modulates the scene spatially. This has applications in various imaging modalities such as spectral, depth, and x-ray imaging [16]. However, the sensing matrix is always considered ideal i.e., binary. However, in practice, the CA is implemented in devices with some non-idealities that attenuate the light such as digital micromirror devices [17]. In other computational optical imaging applications appears this problem such as coded snapshot spectral imaging with coded apertures or with diffractive optical elements [12, 18].

Wireless communications: In multiple-input multiple-output (MIMO) systems we want to recover symbols that are transmitted from linear memoryless channels [2, 19–21]. Before the symbol detection process, a channel estimation method is performed using some transmitted pilot (known) symbols [2]. Usually, the channel estimation contains errors with respect to the ground truth channel leading to a mismatch in the symbol detection algorithm [2]. This phenomenon appears in dynamic communications channels in integrated sensing and communications applications [22, 23].

To address these issues, several works have focused on estimating the unknown sensing operator [12, 24, 25]. This traces back to blind-deconvolution or blind-identification problems [22, 26, 27]. However, jointly estimating the sensing operator and the underlying signal is a highly challenging problem. This work introduces a new

paradigm to address the sensing operator mismatch in deep model-based recovery methods. The proposed method is inspired by the widely used knowledge distillation (KD) technique in deep neural networks [28, 29]. KD was originally introduced to train small and resource-constrained models (student) with the guidance of a, usually pre-trained, big and high-performance model (teacher). The idea is that the teacher can transfer his knowledge to the student to improve his performance (for more details on KD see [29]).

In this work, we extrapolate the KD concept using a model with a fully or almost fully characterized sensing operator (the teacher model). This sensing operator is defined only in simulation, since it may not model the real-world acquisition phenomenon but allows a high reconstruction performance. The student model uses a less characterized sensing operator, i.e., with a partial knowledge or inexact sensing operator, which follows a realistic sensing scenario. The teacher model system serves as a guide for the student model, thereby improving its performance. To transfer the knowledge from the teacher model to the student model we proposed two distillation loss functions, one that matches the gradient steps of the unrolling network at each stage, and the second promotes that the student has similar signal estimation at each stage of the network. Here, different from the traditional KD application in neural networks, the teacher and student models are of the same size, i.e., they have the same number of parameters, the only difference is the sensing operator available in the model. The student model, while matching the teacher in parameters and layers, is limited by its incomplete knowledge of the sensing operator, affecting its performance. This paper reinterprets the KD concept to address this specific problem. We validate this approach in two important applications: computational optical imaging for SPC reconstruction and MIMO detection in wireless communications. For the first one, we consider a teacher model trained with all the ideal or almost-ideal SPC sensing matrix (binary numbers) with the unrolling network described in [30] and the student only has access to the miscalibrated SPC sensing matrix, which is the binary matrix plus additive noise. In the MIMO detection problem, we employed the DetNet architecture [21], where the teacher is the trained DetNet with near-perfect knowledge of the channel state information (CSI) while the student has an inexact knowledge of the CSI.

2. DEEP MODEL-BASED RECOVERY BACKGROUND

Given the success of deep model-based neural networks in recovery tasks, such as unrolling networks, in this work, we use this approach as the backbone of our recovery methods. In general, we want to learn a neural network that uses the sensing operator to map the measurements to the underlying signal $\mathcal{M}_\theta(\cdot) : \mathbb{R}^m \times \mathbb{R}^{m \times n} \rightarrow \mathbb{R}^n$ with parameters θ . The network is trained as

$$\theta^* = \arg \min_{\theta} \mathbb{E}_{\mathbf{x}, \mathbf{y}} [\ell(\mathcal{M}_\theta(\mathbf{y}, \mathbf{A}), \mathbf{x})], \quad (2.1)$$

where $\ell(\cdot, \cdot)$ is the loss function. This problem is solved using off-the-shelf stochastic gradient descent algorithms [13]. Unrolling networks are built as sequential models of L layers, where each layer is interpreted as an iteration of an iterative algorithm as:

$$\mathcal{M}_\theta(\mathbf{y}, \mathbf{A}) = \mathcal{M}_{\theta L}(\mathcal{M}_{\theta L-1}(\cdots \mathcal{M}_{\theta 1}(\mathbf{y}, \mathbf{A}), \mathbf{A}), \mathbf{A}). \quad (2.2)$$

Mainly, we use two different unrolling networks, an alternating direction method of multipliers (ADMM) [31] based network used for the SPC experiments. The second is the DetNet [32] which is an unrolling network inspired by a projected gradient descent method, this network is used for the MIMO detection in the wireless communications application.

2.1. ADMM-Inspired Network for SPC recovery

First, let's define the sensing process for SPC. Here \mathbf{x} is the vectorized image, we only consider grayscale images but it can be extended for

color or spectral images [16]. The rows of the sensing operator are the vectorized coded apertures $\mathbf{a}_i \in \{-1, 1\}^n, i = 1, \dots, m$ leading to $\mathbf{A} = [\mathbf{a}_1, \dots, \mathbf{a}_m]^\top$, where m is the number of snapshots. The ADMM formulation divides the problem (1.1) into small steps. Thus, an auxiliary variable $\mathbf{z} \in \mathbb{R}^n$ is introduced, leading to

$$\underset{\tilde{\mathbf{x}}, \mathbf{z}}{\text{minimize}} \frac{1}{2} \|\mathbf{y} - \mathbf{A}\tilde{\mathbf{x}}\|_2^2 + \lambda g(\mathbf{z}) \quad \text{s.t. } \mathbf{z} = \tilde{\mathbf{x}}. \quad (2.3)$$

To solve this problem for both variables, \mathbf{x} and \mathbf{z} , the augmented Lagrangian is formulated as:

$$L_\rho(\tilde{\mathbf{x}}, \mathbf{z}, \mathbf{u}) = \frac{1}{2} \|\mathbf{y} - \mathbf{A}\tilde{\mathbf{x}}\|_2^2 + \lambda g(\mathbf{z}) + \frac{\rho}{2} \|\mathbf{z} - \tilde{\mathbf{x}} + \mathbf{u}\|, \quad (2.4)$$

where $\rho > 0$ is a penalty parameter, and $\mathbf{u} \in \mathbb{R}^n$ is the Lagrange multiplier. Then, the optimization problem is solved iteratively by updating the variables \mathbf{z} , $\tilde{\mathbf{x}}$, and \mathbf{u} , following

$$\begin{cases} \mathbf{z}^{l+1} & := \arg \min_{\mathbf{z}} \left(g(\mathbf{z}) + \frac{\rho}{2} \|\tilde{\mathbf{x}}^l - \mathbf{z} + \mathbf{u}^l\|_2^2 \right), \\ \tilde{\mathbf{x}}^{l+1} & := \arg \min_{\tilde{\mathbf{x}}} \left(f(\tilde{\mathbf{x}}) + \frac{\rho}{2} \|\tilde{\mathbf{x}} - \mathbf{z}^{l+1} + \mathbf{u}^l\|_2^2 \right), \\ \mathbf{u}^{l+1} & := \mathbf{u}^l + \tilde{\mathbf{x}}^{l+1} - \mathbf{z}^{l+1}. \end{cases} \quad (2.5)$$

To solve the \mathbf{z} -update a neural network $\mathcal{D}_{\beta^l}(\cdot)$ is employed to learn the proximal operator of this term. The $\tilde{\mathbf{x}}$ -update is performed via gradient descent formulation. And finally, the dual variable \mathbf{u} is updated via dual ascent iteration. In Algorithm 1, the unfolding of the ADMM iterations. Highlighted in blue are the learnable parameters at every iteration which are $\theta = \{\beta^l, \alpha^l, \rho^l\}_{l=1}^L$.

2.2. DetNet for MIMO detection

MIMO detection problem refers to recovering the signal $\bar{\mathbf{x}} \in \mathbb{C}^{\bar{n}}$ using the received signal $\bar{\mathbf{y}} \in \mathbb{C}^{\bar{m}}$ and the known channel matrix \mathbf{A} . Let $\bar{\mathbf{A}} \in \mathbb{C}^{\bar{m} \times \bar{n}}$ is the channel matrix with $\bar{m} \leq \bar{n}$ where \bar{n} and \bar{m} are the number of transmitter and receiver antennas. We consider the MIMO system model $\bar{\mathbf{y}} = \bar{\mathbf{A}}\bar{\mathbf{x}} + \bar{\mathbf{w}}$, where $\bar{\mathbf{x}} \in \mathcal{S}^{\bar{n}}$ is a transmitted signal from finite square signal constellation \mathcal{S} , and $\bar{\mathbf{w}} \in \mathbb{C}^{\bar{m}}$ is a Gaussian noise vector. The complex-valued model can be reformulated as the real-valued model $\mathbf{y} = \mathbf{A}\mathbf{x} + \boldsymbol{\omega}$, where

$$\mathbf{y} = \begin{bmatrix} \Re(\bar{\mathbf{y}}) \\ \Im(\bar{\mathbf{y}}) \end{bmatrix}, \mathbf{x} = \begin{bmatrix} \Re(\bar{\mathbf{x}}) \\ \Im(\bar{\mathbf{x}}) \end{bmatrix}, \boldsymbol{\omega} = \begin{bmatrix} \Re(\bar{\mathbf{w}}) \\ \Im(\bar{\mathbf{w}}) \end{bmatrix}, \mathbf{A} = \begin{bmatrix} \Re(\bar{\mathbf{A}}) & -\Im(\bar{\mathbf{A}}) \\ \Im(\bar{\mathbf{A}}) & \Re(\bar{\mathbf{A}}) \end{bmatrix},$$

with $m = 2\bar{m}$ and $n = 2\bar{n}$, therefore the receiver can be rearranged to obtain the equivalent real channel model (2). Where $\mathbf{y} \in \mathbb{R}^m$, $\mathbf{A} \in \mathbb{R}^{m \times n}$, $\mathbf{x} \in \mathcal{S}^n$ and $\mathbf{w} \in \mathbb{R}^m$ are the received signal, the channel matrix, the transmitted signal and the noise, respectively. In this case, $\mathcal{S} = \Re(\bar{\mathcal{S}})$ represent the real part of complex constellations. In the MIMO detection problem, since the underlying signal (symbols) belongs to a defined constellation (BPSK, QPSK, or 16QAM among others), i.e., $\mathbf{x} \in \mathcal{S}^n$, where in the case of BPSK $\mathcal{S} = \{-1, 1\}$. Thus, the optimization problem is formulated as:

$$\underset{\tilde{\mathbf{x}}}{\text{minimize}} \|\mathbf{y} - \mathbf{A}\tilde{\mathbf{x}}\|_2 + I_{\mathcal{S}}(\tilde{\mathbf{x}}), \quad (2.6)$$

where $I_{\mathcal{S}}(\cdot)$ is an element-wise indicator function over the constellation set \mathcal{S} , i.e., $I_{\mathcal{S}}(x) = 0$ if $x \in \mathcal{S}$ and $I_{\mathcal{S}}(x) = \infty$ if $x \notin \mathcal{S}$. Thus, a projected gradient descent (PGD) approach is highly suitable for this problem. Mainly, PGD iteration for (2.6) is

$$\tilde{\mathbf{x}}^{l+1} = \Pi_{I_{\mathcal{S}}} \left(\tilde{\mathbf{x}}^l - \alpha^l \mathbf{A}^\top \left(\mathbf{A}\tilde{\mathbf{x}}^l - \mathbf{y} \right) \right). \quad (2.7)$$

The DetNet improves this algorithm by lifting the gradient step to a higher dimension using fully connected layers and non-linear activation functions. This is followed by two fully connected layers. The summary of the algorithm is shown in Algorithm 2. The function $\varrho(\cdot)$ is the ReLu activation function and the $\psi_t(\cdot) = -1 + \frac{\varrho(+t)}{|t|} - \frac{\varrho(-t)}{|t|}$ is the piecewise linear soft sign operator that works as the proximal operator over the constellation set. Here the trainable parameters are $\theta = \{\mathbf{W}_1^l, \mathbf{b}_1^l, \mathbf{W}_2^l, \mathbf{b}_2^l, \mathbf{W}_3^l, \mathbf{b}_3^l\}_{l=1}^L$.

Algorithm 1 ADMM-Inspired Network

Require: $\mathbf{A}, \mathbf{y}, L$

- 1: $\mathbf{x}^0 = \mathbf{A}^T \mathbf{y}, \mathbf{u}^0 = \mathbf{0},$ ▷ Network input initialization
- 2: **for** $l = 1 : L$ **do**
- 3: $\mathbf{z}^{l+1} := \mathcal{D}_{\beta^{l+1}}(\tilde{\mathbf{x}}^l + \mathbf{u}^l).$ ▷ Auxiliary variable update
 $\hspace{10em} = \nabla f(\tilde{\mathbf{x}}^l)$
- 4: $\tilde{\mathbf{x}}^{l+1} := \tilde{\mathbf{x}}^l - \alpha^{l+1} \left(\mathbf{A}^T \left(\mathbf{A} \tilde{\mathbf{x}}^l - \mathbf{y} \right) - \rho^{k+1} \left(\tilde{\mathbf{x}}^l - \mathbf{z}^{l+1} + \mathbf{u}^l \right) \right)$ ▷ $\tilde{\mathbf{x}}$ -Update
- 5: $\mathbf{u}^{l+1} = \mathbf{u}^l + \mathbf{x}^{l+1} - \mathbf{z}^{l+1}$ ▷ \mathbf{u} -Update

Algorithm 2 MIMO detection network

Require: $\mathbf{A}, \mathbf{y}, L$

- 1: $\mathbf{x}^0 = \mathbf{0}, \mathbf{v}^0 = \mathbf{0},$ ▷ Network input initialization
- 2: **for** $l = 1 : L$ **do**
- 3: $\mathbf{z}^l = \varrho \left(\mathbf{W}_1^l \left[\begin{array}{c} \mathbf{A}^T \mathbf{y} \\ \tilde{\mathbf{x}}^l \\ \mathbf{A}^T \mathbf{A} \tilde{\mathbf{x}}^l \\ \mathbf{v}^l \end{array} \right] + \mathbf{b}_1^l \right)$ ▷ Gradient descent
 $\hspace{10em} = \nabla f(\tilde{\mathbf{x}}^l)$
- 4: $\tilde{\mathbf{x}}^{l+1} = \psi_t(\mathbf{W}_2^l \mathbf{z}^l + \mathbf{b}_2^l)$ ▷ Soft-sign operator
- 5: $\mathbf{v}^{l+1} = \mathbf{W}_3^l \mathbf{z}^l + \mathbf{b}_3^l$ ▷ Lifted variable Update

3. SIGNAL RECONSTRUCTION WITH INEXACT SENSING OPERATOR

Unrolling methods, as described in the previous section, require full knowledge of the sensing operator \mathbf{A} to have optimal reconstruction performance. Here, we consider that the sensing operator is composed as $\mathbf{A} = \mathbf{A}_k + \mathbf{A}_u$, where \mathbf{A}_k is the known portion of the sensing operator and \mathbf{A}_u is the unknown part. In unrolling networks, having only access to an inexact sensing operator affects the fidelity term update since we only have that

$$f(\tilde{\mathbf{x}}) = \|\widehat{\mathbf{y}} - (\mathbf{A}_k + \mathbf{A}_u)\tilde{\mathbf{x}} + \omega\|, \quad (3.1)$$

this mismatch significantly affects the gradient computation of the fidelity term, specifically on line 4 in Algorithm 1 and line 5 in Algorithm 2, since the direction of the gradient leads to the wrong optimization direction. Additionally, if the power of the unknown matrix \mathbf{A}_u is significantly higher than the power of the known sensing matrix the performance drop is higher. Here we consider that the unknown sensing operator is a random variable, where each entry is i.i.d from a Gaussian distribution $[\mathbf{A}_u]_{i,j} \sim \mathcal{N}(0, \sigma^2)$. Here, the power of the unknown sensing operator is directly proportional to the variance σ^2 . As a proof-of-concept of this issue, we validate on both applications (MIMO detection and SPC recovery) the effect of the power of the unknown sensing matrix in the models' performance. First, for the MIMO detection, we run the DetNet model (Algorithm 2) for different variances of the unknown signal and plot the bit error rate (BER, the lower the better) of the recovered BPSK signal and for different signal-to-noise-ratio (SNR) in the measurements. The results shown in Fig. 1a) confirm the significant decrease in the inexact channel matrix performance. Similarly, for the SPC recovery, the ADMM network model (Algorithm 1), using the peak-signal-to-noise-ratio (PSNR, the higher to better) and the structural similarity index measure (SSIM, the closer to one the better) for various values of σ . The results show a decrease of up to 14 [dB] in the PSNR for $\sigma = 0.9$ with respect to the ideal case. To address this issue, we propose a new learning approach to train the unrolling network using the mismatched fidelity term (3.1).

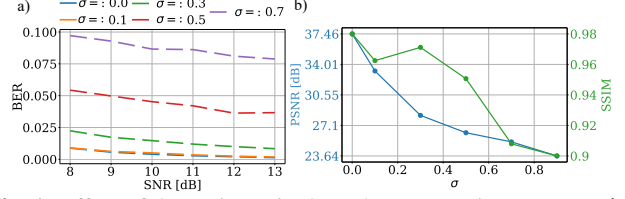


Fig. 1. Effect of the variance in the unknown sensing operator \mathbf{A}_u for a) deep MIMO detection with DetNet and b) SPC recovery with ADMM-Inspired network.

3.1. Teacher structure

Here we define the teacher as synthetic since we only have access to it in simulation. Thus, let $\mathbf{A}_t = \mathbf{A}_k + \mathbf{A}_{ut}$ be the sensing matrix, where the entries of unknown operator \mathbf{A}_{ut} also follows a Gaussian distribution $[\mathbf{A}_{ut}]_{i,j} \sim \mathcal{N}(0, \sigma_t^2)$ where σ_t^2 is the variance of the teacher, which satisfies that $0 \leq \sigma_t^2 < \sigma^2$. Note that the known matrix \mathbf{A}_k is the same for the student and teacher system, the only difference relies on the variance of the unknown matrices. The corresponding measurements are $\mathbf{y}_t = \mathbf{A}_t \mathbf{x} + \omega$. The teacher model is trained based on the equation (2.1) with paired dataset $\{\mathbf{y}_t, \mathbf{x}\}$ leading to $\mathcal{M}_{\theta_t^*}(\mathbf{y}_t, \mathbf{A}_k)$. Note, that in every iteration this network has access to the exact or almost-exact sensing operator since it has the structure of equation (2.2) which can lead to a better recovery performance (see Figure 1 in lower values of σ). In the proposed method, we can control the quality of the teacher by setting the parameter σ_t , thus this is a hyperparameter of the method.

3.2. Distillation Loss Function

To distill the knowledge of the teacher model to the student model, we propose to regularize the optimization of the student. Before introducing the proposed optimization problem, we introduce the following variables: the estimations at each stage of the student and teacher unrolling networks are denoted as $\tilde{\mathcal{X}}_s = \{\tilde{\mathbf{x}}_s^1, \dots, \tilde{\mathbf{x}}_s^L\}$ and $\tilde{\mathcal{X}}_t = \{\tilde{\mathbf{x}}_t^1, \dots, \tilde{\mathbf{x}}_t^L\}$. On the other hand, we define the collection of the data fidelity gradient at each stage for the student and teacher models as $\mathcal{G}_s = \{\nabla f(\tilde{\mathbf{x}}_s^1), \dots, \nabla f(\tilde{\mathbf{x}}_s^L)\}$ and $\mathcal{G}_t = \{\nabla f(\tilde{\mathbf{x}}_t^1), \dots, \nabla f(\tilde{\mathbf{x}}_t^L)\}$. Thus, the proposed optimization is

$$\theta^* = \arg \min_{\theta} \mathbb{E}_{\mathbf{x}, \mathbf{y}, \mathbf{y}_t} [\mathcal{L}(\mathcal{M}_{\theta}(\mathbf{y}, \mathbf{A}_k), \mathbf{x}, \mathcal{M}_{\theta_t^*}(\mathbf{y}_t, \mathbf{A}_k))] \quad (3.2)$$

$$\mathcal{L} = \ell(\mathcal{M}_{\theta}(\mathbf{y}, \mathbf{A}_k), \mathbf{x}) + \ell_{KD}(\mathcal{M}_{\theta}(\mathbf{y}, \mathbf{A}_k), \mathcal{M}_{\theta_t^*}(\mathbf{y}_t, \mathbf{A}_k)),$$

where the distillation loss is composed of two terms, one comparing the gradients of the student and teacher models and the other comparing their outputs. Then, distillation loss is

$$\ell_{KD} = \lambda_{grad} \ell_{grad}(\mathcal{G}_s, \mathcal{G}_t) + \lambda_o \ell_o(\tilde{\mathcal{X}}_s, \tilde{\mathcal{X}}_t), \quad (3.3)$$

where λ_{grad} and λ_o are hyperparameters. Both loss functions are defined as

$$\ell_{grad}(\mathcal{G}_s, \mathcal{G}_t) = \sum_{i=1}^L \log(i) \|\nabla f(\tilde{\mathbf{x}}_s^i) - \nabla f(\tilde{\mathbf{x}}_t^i)\|_2, \quad (3.4)$$

$$\ell_o(\tilde{\mathcal{X}}_s, \tilde{\mathcal{X}}_t) = \sum_{i=1}^L \log(i) \|\tilde{\mathbf{x}}_s^i - \tilde{\mathbf{x}}_t^i\|_2. \quad (3.5)$$

The main idea behind these loss functions is to guide the student's data fidelity gradient since the inexact sensing operator significantly affects this term. The output loss function guides the recovery at every iteration. An overview of the proposed method is shown in Fig. 2. This approach involves higher computational costs during the student training phase, as it requires storing, performing inference, and pre-training the teacher model. However, only the student model is utilized during inference, ensuring that real-world deployment does not incur additional computational overhead.

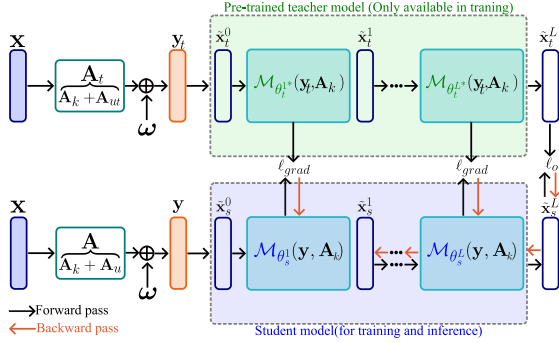


Fig. 2. Scheme of the proposed optimization paradigm based on KD. The teacher model (green) consists of an unrolling network pre-trained with full or almost full knowledge of the sensing operator. In contrast, the student model (blue) consists of an unrolling network with the same architecture as the teacher’s. However, the student only has access to partial knowledge of the sensing operator.

4. EXPERIMENTS & RESULTS

The effectiveness of the proposed approach was validated through several experiments in two key applications: SPC recovery and wireless communication via MIMO detection. The source code can be found in [33]. The source code was developed in PyTorch framework [34]. In all the results, the baseline is the student trained without the distillation loss functions.

SPC recovery: The MNIST dataset, consisting of 60,000 training images resized to 32×32 across, was used for training. The dataset was divided into 50,000 images for training and 10,000 for validation. The test set contains 10,000 images. The unrolling network comprises $L = 10$ stages and was trained for 50 epochs using the Adam optimizer [35] with a learning rate of $5e^{-4}$ and a batch size of 600 images. In this experiment, the known binary sensing matrix rows are the rows of the Hadamard basis using the cake-cutting ordering. The matrix was generated using the algorithm proposed in [36]. The parameters of the distillation loss functions were set to $\lambda_{grad} = \lambda_o = 1e^{-3}$. We used the mean-squared error (MSE) for the reconstruction loss function. We consider training several teacher models with different $\sigma_t = \{0.0, 0.1, 0.5, 0.7\}$ to validate our proposed method in this application. Then, to train the student model, we consider $\sigma = \{0.3, 0.5, 0.7, 0.9\}$ and perform the training for each teacher model that satisfies that $\sigma > \sigma_t$. The result of this experiment is shown in Fig 3. Particularly, in Fig 3a) quantitative results are shown with a recovery performance mean of 10 repetitions, wherein each repetition new random unknown matrices \mathbf{A}_u and \mathbf{A}_{ut} are generated. The results show that the proposed KD approach improves the recovery PSNR by up to 1.5[dB] in $\sigma = 0.3$ and 0.5 [dB] in $\sigma = 0.9$. Another observation is that the best performance for each σ is not always the best teacher (the model with smaller σ_t) suggesting that we require a teacher with not too high performance to guide the student’s training properly. In Fig 3b) is shown visual results of the proposed method and the baseline where the proposed method achieves better reconstruction quality for each value of σ .

MIMO detection: The DetNet was trained for 1,000 iterations. We set the number of transmitters to $n = 30$ and the number of received antennas to $m = 60$. The number of stages was set $L = 90$. In each iteration, random binary BPSK signals were generated along with the channel matrix which follows a Gaussian distribution. A batch size of 5,000 signals was used, and the additive Gaussian noise ω with an SNR value sampled from a uniform distribution between 7 db and 13 db. Here the distillation losses hyperparameters were set to $\lambda_o = \lambda_{grad} = 1e^{-2}$. The recovery loss is the one used in the original

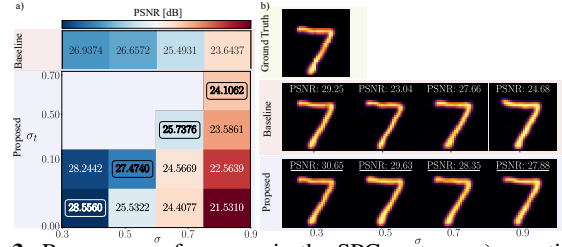


Fig. 3. Recovery performance in the SPC system. a) quantitative results for different values of σ_t and σ . b) Visual reconstruction for the best-performing configuration of the method and the baseline

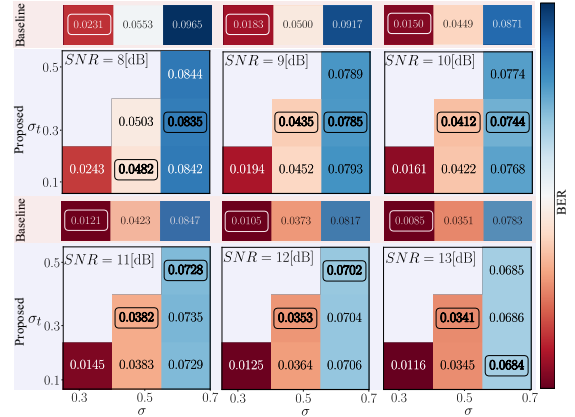


Fig. 4. Detection performance in MIMO systems for different values of for the proposed method σ_t and σ and varying the SNR .

DetNet paper [21]. A linear-decay learning rate schedule was used, starting from $0.9e^{-3}$ with a decay factor of 0.97 every 50 iterations. As in the first experiment, we study the effect of the values of σ and σ_t in the proposed method and compare them with the baseline. The results are shown in 4 where for different values of SNR in testing is displayed the detection BER of every configuration. The proposed method outperforms the baselines in the most challenging scenarios, with values of $\sigma \leq 0.5$. For $\sigma = 0.3$ the baseline is better, however, this is because for this small value of σ the detection performance is not significantly affected compared with the exact sensing operator model ($\sigma = 0$ in Fig. 1a)). Note that the best teacher setting for the student is not always the best-performing student.

5. CONCLUSIONS

A new recovery paradigm based on KD was proposed to address signal recovery methods with inexact sensing operators. This method leverages a system with a synthetic fully or nearly fully characterized sensing operator as the teacher model, which achieves high signal reconstruction performance. The teacher then transfers his knowledge to a system with a less characterized sensing operator, the student, using two distillation loss functions. Experimental results in SPC and MIMO detection validate the method’s effectiveness. An important aspect of the proposed method is the teacher setting, where a high-performing teacher does not necessarily deliver a good knowledge transfer to the student. Future works will be focused on the teacher’s design for optimal knowledge transfer. Furthermore, this approach can be incorporated into models that address signal reconstruction with inexact sensing operators [37, 38] to enhance the quality and robustness of the reconstruction.

6. REFERENCES

- [1] Z. Qin, H. Ye, G. Y. Li, and B.-H. F. Juang, "Deep learning in physical layer communications," *IEEE Wireless Communications*, vol. 26, no. 2, pp. 93–99, 2019.
- [2] H. He, C.-K. Wen, S. Jin, and G. Y. Li, "Model-driven deep learning for mimo detection," *IEEE Transactions on Signal Processing*, vol. 68, pp. 1702–1715, 2020.
- [3] H. He, S. Jin, C.-K. Wen, F. Gao, G. Y. Li, and Z. Xu, "Model-driven deep learning for physical layer communications," *IEEE Wireless Communications*, vol. 26, no. 5, pp. 77–83, 2019.
- [4] E. McLeod and A. Ozcan, "Unconventional methods of imaging: computational microscopy and compact implementations," *Reports on Progress in Physics*, vol. 79, no. 7, p. 076001, 2016.
- [5] A. Shajkofci and M. Liebling, "Spatially-variant cnn-based point spread function estimation for blind deconvolution and depth estimation in optical microscopy," *IEEE Transactions on Image Processing*, vol. 29, pp. 5848–5861, 2020.
- [6] R. Lukac, *Computational photography: methods and applications*. CRC press, 2017.
- [7] B. I. Erkmén, "Computational ghost imaging for remote sensing," *JOSA A*, vol. 29, no. 5, pp. 782–789, 2012.
- [8] B. Jin, P. Maaß, and O. Scherzer, "Sparsity regularization in inverse problems," *Inverse Problems*, vol. 33, no. 6, 2017.
- [9] S. Osher, M. Burger, D. Goldfarb, J. Xu, and W. Yin, "An iterative regularization method for total variation-based image restoration," *Multiscale Modeling & Simulation*, vol. 4, no. 2, pp. 460–489, 2005.
- [10] W. Dong, G. Shi, X. Li, Y. Ma, and F. Huang, "Compressive sensing via nonlocal low-rank regularization," *IEEE transactions on image processing*, vol. 23, no. 8, pp. 3618–3632, 2014.
- [11] Y. Yang, J. Sun, H. Li, and Z. Xu, "Admm-csnet: A deep learning approach for image compressive sensing," *IEEE transactions on pattern analysis and machine intelligence*, vol. 42, no. 3, pp. 521–538, 2018.
- [12] R. Gualdrón-Hurtado, H. Arguello, and J. Bacca, "Deep learned non-linear propagation model regularizer for compressive spectral imaging," *IEEE Transactions on Computational Imaging*, 2024.
- [13] V. Monga, Y. Li, and Y. C. Eldar, "Algorithm unrolling: Interpretable, efficient deep learning for signal and image processing," *IEEE Signal Processing Magazine*, vol. 38, no. 2, pp. 18–44, 2021.
- [14] Z. Zhao, T. Li, B. An, S. Wang, B. Ding, R. Yan, and X. Chen, "Model-driven deep unrolling: Towards interpretable deep learning against noise attacks for intelligent fault diagnosis," *ISA transactions*, vol. 129, pp. 644–662, 2022.
- [15] N. Shlezinger, J. Whang, Y. C. Eldar, and A. G. Dimakis, "Model-based deep learning," *Proceedings of the IEEE*, vol. 111, no. 5, pp. 465–499, 2023.
- [16] G. M. Gibson, S. D. Johnson, and M. J. Padgett, "Single-pixel imaging 12 years on: a review," *Optics express*, vol. 28, no. 19, pp. 28 190–28 208, 2020.
- [17] H. Garcia, J. Bacca, B. Wohlberg, and H. Arguello, "Calibration reinforcement regularizations for optimized snapshot spectral imaging," *Applied Optics*, vol. 62, no. 8, pp. C135–C145, 2023.
- [18] L. Li, L. Wang, W. Song, L. Zhang, Z. Xiong, and H. Huang, "Quantization-aware deep optics for diffractive snapshot hyperspectral imaging," in *Proceedings of the IEEE/CVF Conference on Computer Vision and Pattern Recognition*, 2022, pp. 19 780–19 789.
- [19] K. Zheng, L. Zhao, J. Mei, B. Shao, W. Xiang, and L. Hanzo, "Survey of large-scale mimo systems," *IEEE Communications Surveys & Tutorials*, vol. 17, no. 3, pp. 1738–1760, 2015.
- [20] S. Solano, R. Jacome, E. Vargas, and H. Arguello, "Data-driven based preconditioning for one-bit mimo detection," in *2024 XXIV Symposium of Image, Signal Processing, and Artificial Vision (STSIVA)*. IEEE, 2024, pp. 1–5.
- [21] N. Samuel, T. Diskin, and A. Wiesel, "Deep mimo detection," in *2017 IEEE 18th International Workshop on Signal Processing Advances in Wireless Communications (SPAWC)*. IEEE, 2017, pp. 1–5.
- [22] E. Vargas, K. V. Mishra, R. Jacome, B. M. Sadler, and H. Arguello, "Dual-blind deconvolution for overlaid radar-communications systems," *IEEE Journal on Selected Areas in Information Theory*, vol. 4, pp. 75–93, 2023.
- [23] R. Jacome, E. Vargas, K. V. Mishra, B. M. Sadler, and H. Arguello, "Multi-antenna dual-blind deconvolution for joint radar-communications via soman minimization," *Signal Processing*, vol. 221, p. 109484, 2024.
- [24] L. Song, L. Wang, M. H. Kim, and H. Huang, "High-accuracy image formation model for coded aperture snapshot spectral imaging," *IEEE Transactions on Computational Imaging*, vol. 8, pp. 188–200, 2022.
- [25] S. Campo, K. Fonseca, H. Garcia, and H. Arguello, "Point spread function estimation using principal component analysis for a double diffractive optical element system," in *2024 XXIV Symposium of Image, Signal Processing, and Artificial Vision (STSIVA)*. IEEE, 2024, pp. 1–5.
- [26] D. Ren, K. Zhang, Q. Wang, Q. Hu, and W. Zuo, "Neural blind deconvolution using deep priors," in *Proceedings of the IEEE/CVF conference on computer vision and pattern recognition*, 2020, pp. 3341–3350.
- [27] A. Ahmed, B. Recht, and J. Romberg, "Blind deconvolution using convex programming," *IEEE Transactions on Information Theory*, vol. 60, no. 3, pp. 1711–1732, 2013.
- [28] G. Hinton, "Distilling the knowledge in a neural network," *arXiv preprint arXiv:1503.02531*, 2015.
- [29] J. Gou, B. Yu, S. J. Maybank, and D. Tao, "Knowledge distillation: A survey," *International Journal of Computer Vision*, vol. 129, no. 6, pp. 1789–1819, 2021.
- [30] L. Suarez-Rodriguez, R. Jacome, and H. Arguello, "Highly constrained coded aperture imaging systems design via a knowledge distillation approach," *arXiv e-prints*, pp. arXiv–2406, 2024.
- [31] S. Boyd, N. Parikh, E. Chu, B. Peleato, J. Eckstein *et al.*, "Distributed optimization and statistical learning via the alternating direction method of multipliers," *Foundations and Trends® in Machine learning*, vol. 3, no. 1, pp. 1–122, 2011.
- [32] Z. Li, C. Peng, G. Yu, X. Zhang, Y. Deng, and J. Sun, "Detnet: Design backbone for object detection," in *Proceedings of the European conference on computer vision (ECCV)*, 2018, pp. 334–350.
- [33] [Online]. Available: https://github.com/leonsuarez24/KD_CALIBRATION.git
- [34] A. Paszke, S. Gross, F. Massa, A. Lerer, J. Bradbury, G. Chanan, T. Killeen, Z. Lin, N. Gimelshein, L. Antiga *et al.*, "Pytorch: An imperative style, high-performance deep learning library," *Advances in neural information processing systems*, vol. 32, 2019.
- [35] D. P. Kingma and J. Ba, "Adam: A method for stochastic optimization," in *3rd International Conference on Learning Representations, ICLR 2015, San Diego, CA, USA, May 7-9, 2015, Conference Track Proceedings*, Y. Bengio and Y. LeCun, Eds., 2015.
- [36] B. Monroy and J. Bacca, "Hadamard row-wise generation algorithm," 2024. [Online]. Available: <https://arxiv.org/abs/2409.02406>
- [37] W. Pu, C. Zhou, Y. C. Eldar, and M. R. Rodrigues, "Robust learned shrinkage-thresholding (rest): Robust unrolling for sparse recover," *arXiv preprint arXiv:2110.10391*, 2021.
- [38] H. Qian, H. Ling, and X. Lu, "Robust unrolled network for lensless imaging with enhanced resistance to model mismatch and noise," *Optics Express*, vol. 32, no. 17, pp. 30 267–30 283, 2024.